

# Fracture behavior modeling of a 3D crack emanated from bony inclusion in the cement PMMA of total hip replacement

Cherfi Mohamed\*, Sahli Abderahmane and Smail Benbarek

Department of Mechanical Engineering, Laboratory Mechanics Physics of Materials (LMPM),  
University of Sidi Bel Abbes, BP 89, cite Ben M'hidi, Sidi Bel Abbes, 22000, Algeria

(Received May 31, 2017, Revised January 2, 2017, Accepted January 3, 2018)

**Abstract.** In orthopedic surgery and in particular in total hip arthroplasty, the implant fixation is carried out using a surgical cement called polymethylmethacrylat (PMMA). This cement has to insure a good adhesion between implant and bone and a good load distribution to the bone. By its fragile nature, the cement can easily break when it is subjected to a high stress gradient by presenting a craze zone in the vicinity of inclusion. The focus of this study is to analyze the effect of inclusion in some zone of cement in which the loading condition can lead to the crack opening leading to their propagation and consequently the aseptic loosening of the THR. In this study, the fracture behavior of the bone cement including a strange body (bone remain) from which the onset of a crack is supposed. The effect of loading condition, the geometry, the presence of both crack and inclusion on the stress distribution and the fracture behavior of the cement. Results show that the highest stresses are located around the sharp tip of bony inclusion. Most critical cracks are located in the middle of the cement mantle when they are subjected to one leg standing state loading during walking.

**Keywords:** finite element method; total hip replacement; bone cement; biomechanics; bony inclusion; stress intensity factor; submodeling technique

## 1. Introduction

The implantation of total hip prosthesis in the human body is a surgical intervention, which requires medical accuracy and more important to that the reliability of total hip prosthesis's components Naudin and Grumbach (2007), and Pauwels (1973). To ensure a good functionality of the cement to reach its expected target (long lifespan); the analysis of the cement is primordial to determine the zones where the crack can appear Merckx (1993), and Tong and Wong (2003). The arthroplasty is an operation intended to get back the mobility of the articulation, muscle forces, ligaments and other structures constituting the human tissue, which control this articulation by creating a new articular space. It has a target to release the patient from a debilitating pain, bring back a movement and sometime corrects a malformation Huiskes (1993). In the THR, the prosthesis may be sealed with cement or without cement to the bone. In this study, we are interested in the cemented total hip replacement (THR). The acrylic bone cement (PMMA) used in orthopedic surgery (in the mechanical point of view) is the weakest element in the load transfer chain: stem-cement-bone. So, this material is the first responsible of the lifespan of the THR Merckx (2003). In order to increase the life of the THR, the study of this material's behavior is become primordial to get an excellent quality of the THR. The cement of THR systematically have to resist to stresses generated by the mechanical effort

of different movement of the human body during his daily movements. This type of stresses leads to the growth of small cracks and then the fracture of the cement Cherfi *et al.* (2016a, b), Benbarek *et al.* (2013a, b), and Jasty *et al.* (1991a, b), and Ouinas *et al.* (2009a, b).

Several works focus on the behavior in break either by the method of the finite elements FEM, or by the XFEM method, the aim of which is to characterize the material whatever by a static or cyclic loading, we can cite for example: Zagane *et al.* (2016a, b), and Omidi *et al.* (2014a, b), and Nanda Kumar *et al.* (2016a, b), and Jiang *et al.* (2014a, b).

Several authors have taken this path of study, the purpose of which is to know the fracture behavior of the (PMMA) cement, the determining material of the PTH one can quote for example: Benouis *et al.* (2015a, b) and Bouziane *et al.* (2016a, b), and Serier *et al.* (2016a, b) and Bouziane *et al.* (2016a, b)

The target of this study is to analyze the fracture behavior of the cement when it included a bone remain as inclusion. For the purpose one supposes the existence of a microscopic crack emanating from a bony inclusion. In this study one, suppose that the cement includes a bone fragment and it has a pyramidal type shape with sharp angle and take a finite volume. The target is to show the effect of the presence of the impurity and a crack on the fracture behavior of the cement.

One chooses three different orientations defined by the following inclination  $0^\circ$ ;  $+23^\circ$  et  $-23^\circ$ , which reproduce the human body posture. The analyzes is done using the finite element method using Abaqus software Yoshidaa *et al.* (2009a, b), and Abaqus 6.11 Documentation. This analysis

\*Corresponding author, Ph.D.  
E-mail: [mouh\\_cherfi@hotmail.fr](mailto:mouh_cherfi@hotmail.fr)

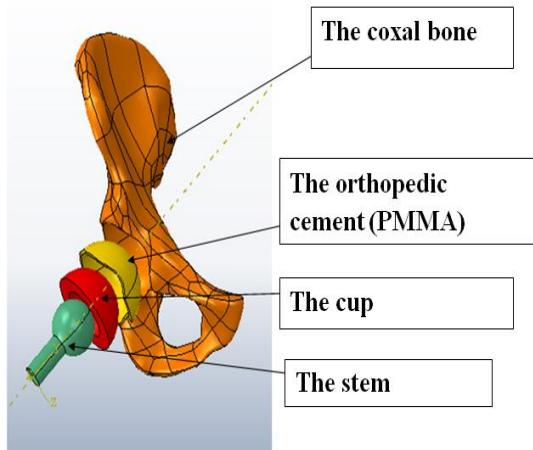


Fig. 1 The constituent elements of the THR

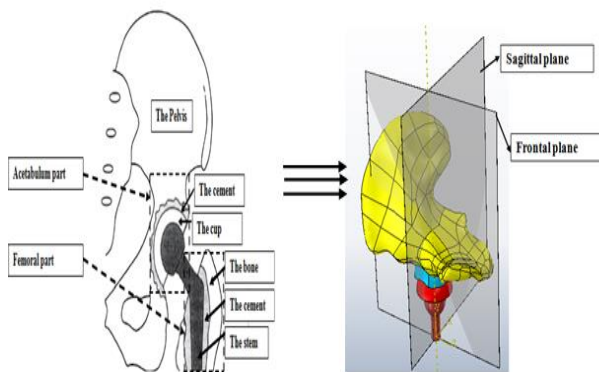


Fig. 2 Geometrical model with sagittal and frontal pla

has done on the acetabulum part of the THR. One study the fracture behavior of the PMMA sealing cement under the effect of 7 times the average human body weight. This represents the case of the stumbling effort during walking functionality Pustoch *et al.* (2009a, b). For this purpose, one calculates the stress intensity factor on the crack front of an emanating crack from an inclusion in the orthopedic cement Maloney *et al.* (1989a, b). In this study, one supposes the existence of a triangular crack of  $100\ \mu\text{m}$  of length. This study treats firstly; the presence effect of an inclusion on the stress distribution, the effect of the applied load and the position of the crack which presents a risk on the cement, and the implant orientation.

## 2. Modeling

### 2.1 geometrical model

The obtaining of the 3D solid model of the patient consists to take images of the interested area using the medical image technique (CT-scan). From these images, one designed this geometrical model using both softwares Solidworks and Amira. The cement has a uniform 2 mm of thickness around acetabulum Benbarek *et al.* (2007a, b) and Benbarek *et al.* (2006a, b), and Poitout (2010).

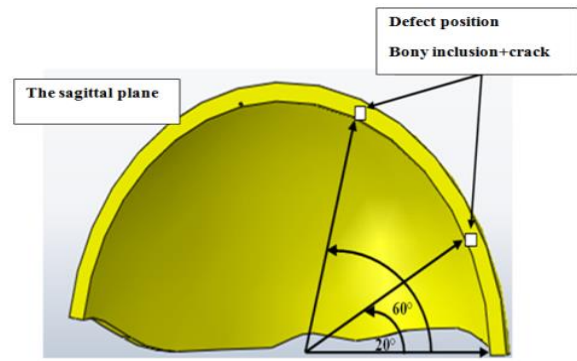


Fig. 3 Inclusion positions in the circumferential system

Fig. 1 shows the three-dimensional geometrical model used in this study, it includes the femoral implant, the orthopedic cement, the cup and the acetabulum bone. The whole system called the total hip prosthesis.

The sagittal plane cuts the THP as shown in Fig. 2. In this plane the crack will be studied in several positions as shows in Fig. 3.

### 2.2 Material model

The material proprieties are taken from different studies Benbarek *et al.* (2007a, b), and Bergman (1990). The below table shows the material properties of different components of the THR.

Materials	Module of Young E (MPa)	Poisson Coefficient $\nu$
coxal bone	17000	0.30
Cup	690	0.30
Cement (PMMA)	2000	0.30
Metallic stem	210000	0.30

### 2.3 Loading model

Several studies were carried out in this field as Pawels (1973). They found that the maximum force acting on the stem head is three times the human body weight Benbarek *et al.* (2007a, b). Other studies carried out on 9 ordinary activities show that the force acting on the stem head is 300% the human body weight Poitout (2010).

Fig. 4 shows the boundary conditions applied on the THR model:

- The sacroiliac joint is fully fixed.
- The pubic joint is allowed to move in sagittal plane.
- A uniformly distributed load of 20 Mpa on the stem neck Benbarek *et al.* (2013, 2007a, b).

In this study we took a load in the case of a stumbling patient. This act generates a load of 7 times of a 70 kg human body weighs. Contacts between the various components of the THR are considered as stiff and continuous Pustoch *et al.* (2009a, b).

3 stem neck positions are taken to represent the three-human body walking posture:  $0^\circ$  and two inclination  $+23^\circ$ ,

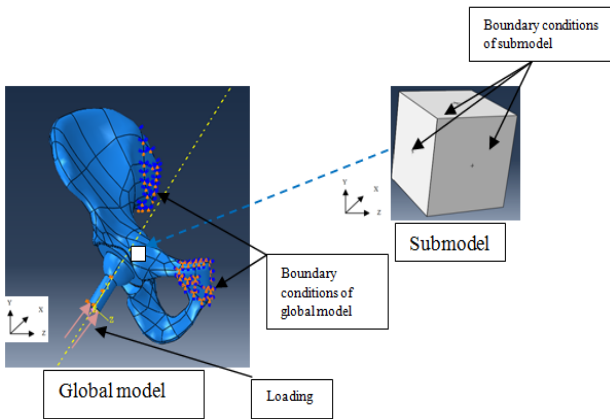


Fig. 4 Schematic of the boundary conditions imposed on the studied structure model (THR)

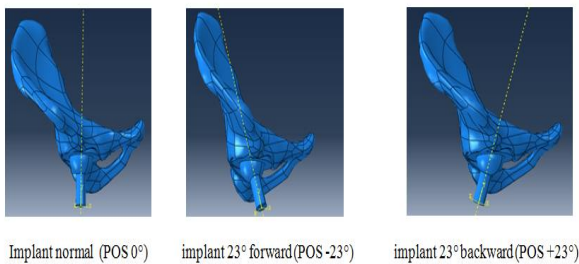


Fig. 5 Three positions of the femoral implant

and  $-23^\circ$  Yoshidaa *et al.* (2004a, b).

### 2.4 Mesh model

The reliability of the obtained results requires a refined mesh. In fact, the cement is a determining element of the prosthesis. The refinement of this mesh is very important for a good analysis of the structure.

In this study we used:

- 6904 quadratic tetrahedron elements have been generated on the implant (metallic stem).
- 8526 quadratic tetrahedron elements have been generated on the cup.
- 6964 quadratic tetrahedron elements have been generated on the coxal bone
- 150400 quadratic trahedron elements have been generated on the cement (PMMA).

The Fig. 6 shows the mesh of the different components of the THR.

The Fig. 7 shows the mesh of the studied area.

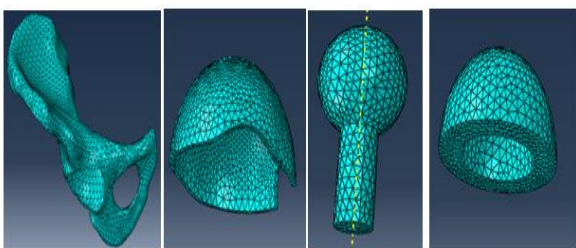


Fig. 6 Meshing of the analyzed prosthesis

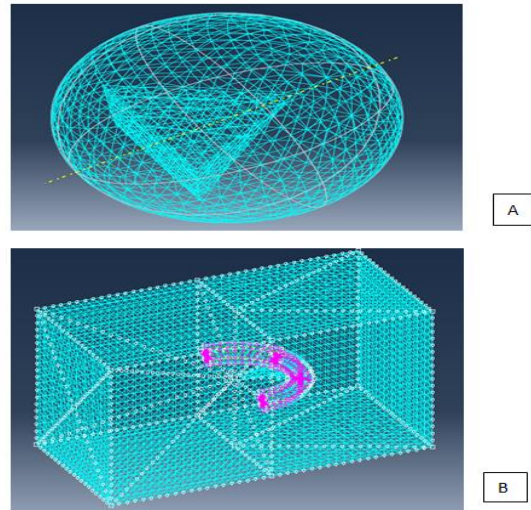


Fig. 7 The mesh model: A): Mesh around the inclusion. B): Mesh of the around the crack front

We opted for three orientations defined by inclinations  $0^\circ$ ,  $25^\circ$  and  $50^\circ$ . They reflect the posture of the human body (Fig. 5).

The quadratic tetraedric type meshing whose number of elements reached 5415 uses for the meshing of bony inclusion, a linear hexaedric with 3680 element used for the meshin of the crack.

### 2.5 Submodeling technique

Submodeling technique is a powerful tool generated by abaqus Software, to analyze physical and thermal phenomenon, and deduce several physical data as: stress, strain, SIF and temperature distribution.

In this study we are interested to calculate the stress intensity factor on the crack front emanating from an inclusion Sahli *et al.* (2014a, b).

We analyze first of all the global model to get the displacements response. In the submodel, the displacements from the global model are applied on the submodel nodes and then get the response of the submodel to these displacements Abaqus 6.11 Documentation (2011).

Fig. 8 shows a schematic representation explaining the submodeling technique using both global and submodel.

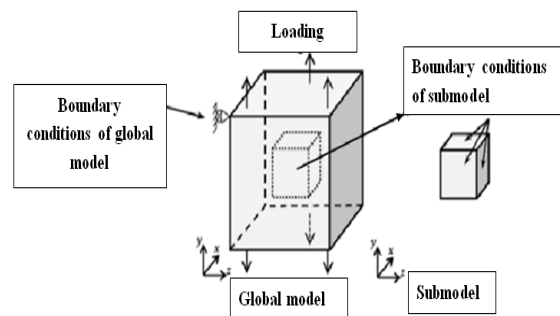


Fig. 8 Schematic representation of the submodeling technique

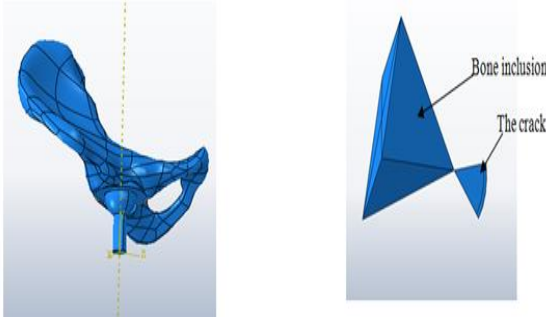


Fig. 9 The global model and the submodel of the studied THR

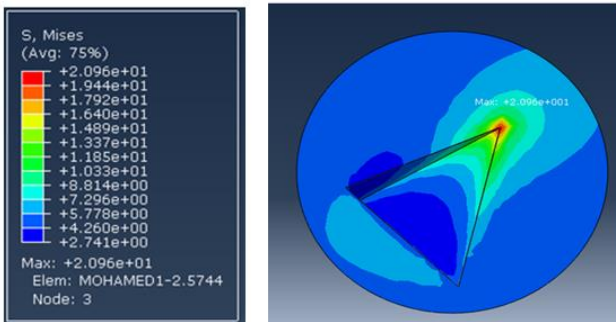
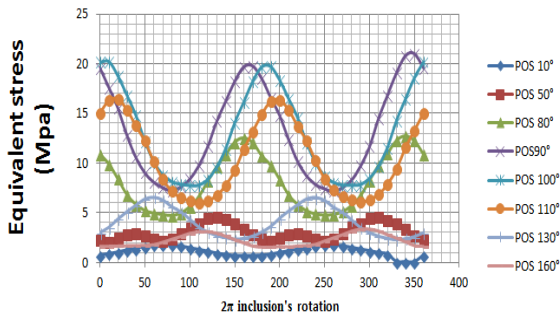


Fig. 10 The variation of the equivalent stress as function of the orientation of the inclusion ( $2\pi$ ) in the circumferential positions (Implant normal)

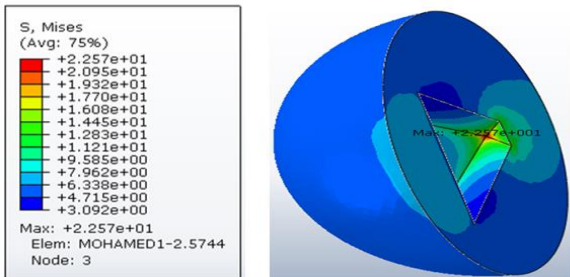
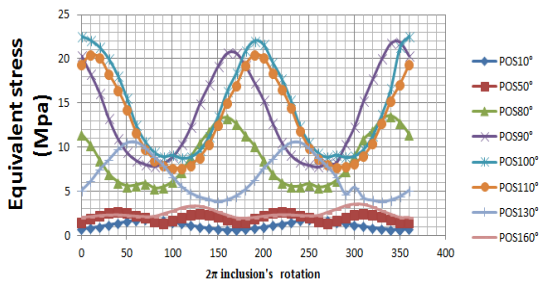


Fig. 11 The variation of the equivalent stress as function of the orientation of the inclusion ( $2\pi$ ) in the circumferential positions (Implant 23° backward)

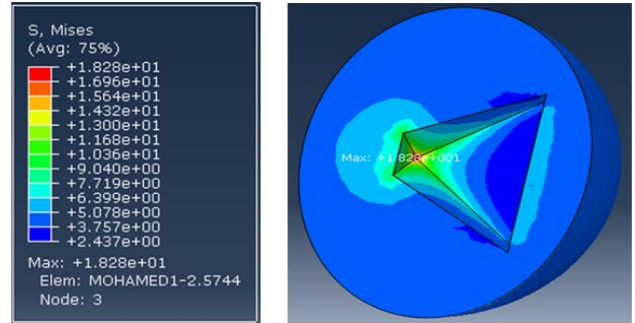
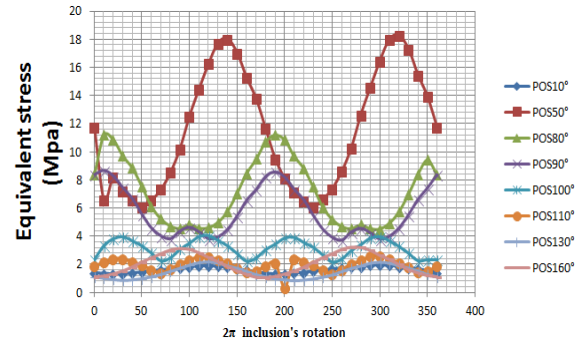


Fig. 12 The variation of the equivalent stress as function of the orientation of the inclusion ( $2\pi$ ) in the circumferential positions (Implant 23° forward)

Fig. 9 shows both global and submodel used in this study.

### 3. Analysis and results

#### 3.1 Effect of the inclusion inclination on the stress distribution

Figs. 10-11 and 12 shows the equivalent stress on the tip of the bony inclusion with respect to the inclusion inclination and the position of inclusion for each Fig. stem position.

In the three graphs, one can notice that there is an inclination which to ward it, the inclusion increases strongly the stress around the inclusion's tip. These inclinations are the radial direction and the anti-radial direction ( $0^\circ$  and  $180^\circ$ ). These cases are critical when the position of the inclusion is in the way of the acting force. These inclinations can lead to a high stress in the cement around the inclusion type.

Fig. 11 shows the most important inclusion position and the three inclinations in which one register the highest stresses on the cement around the inclusion tip. The  $+23^\circ$  human body position is the most critical body position, which makes the cement under great sollicitation. The stress can reach easily 23 MPa under this body posture when the inclusion is favourably oriented (toward radial direction in the polar coordinate system one remained that the yield stress of the cement is about 27 Mpa).

#### 3.2 Behaviour in crack of the cement PMMA

In the present simulation, one supposes the presence of the strange body (body inclusion) in the sealing cement of

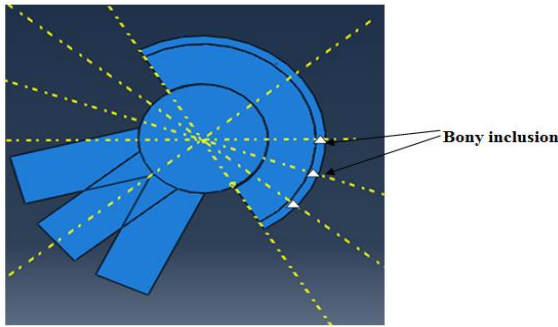


Fig. 13 The positions of the bony inclusion and implant positions

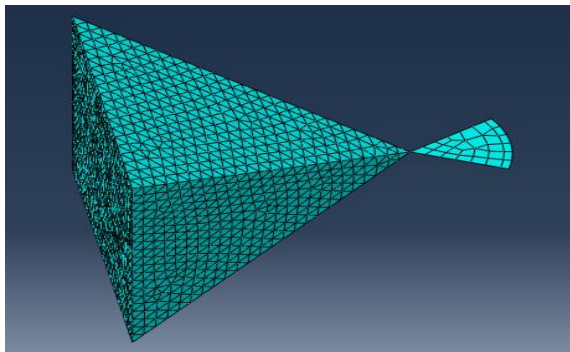


Fig. 14 The Geometry and the meshing of the set submodel

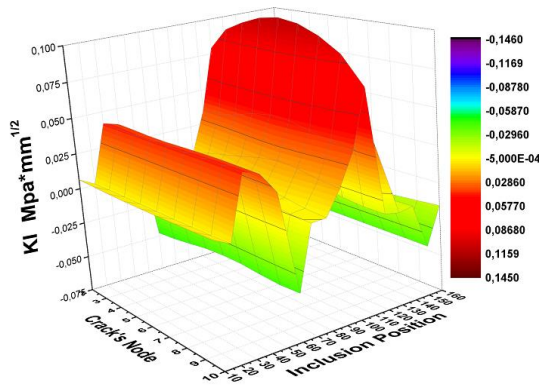


Fig. 15 Distribution of the KI along the crack front according to the inclusion position (Implant Normal)

the THR, the crack front ahead of the inclusion tip is showed in Fig. 14, one calculates all stress intensity factors (SIF): KI, KII and KIII on the crack front with respect to the inclusion inclination and its position as showed in Fig. 13.

Figs. 15-16 and 17 show the variation of the SIF along the crack front with respect to the inclusion orientation for the first position of stem.

The graphs present the variation of stress intensity factor according to the circumferential positions of defect under the three-loading type.

One notice on these Fig. that the mode I SIF is instable for the three loading type (0°, +23°, and -23°), the 10° and 80° positions do not present any risk of fracture due to the K1 values (about 0,04)  $Mpa\sqrt{mm}$ , the circonfereential direction in the polar system (130°) gives the weakest K1

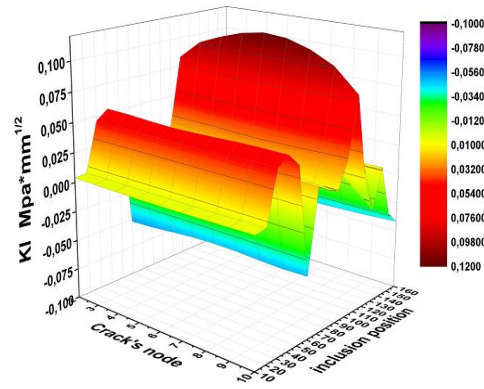


Fig. 16 Distribution of the KI along the crack front according to the inclusion position (Implant 23° behind)

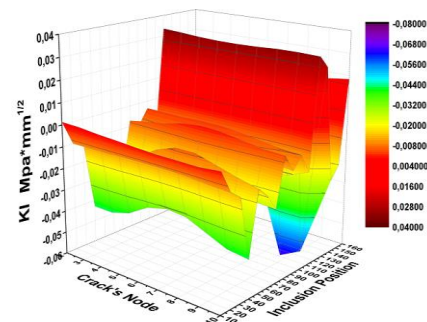


Fig. 17 Distribution of the KI along the crack front according to the inclusion position (Implant 23° forward)

values (0,064 .0,025) consequently for the 1st and 2nd load position.

One notices that the negative SIF values mean that the crack is closed and positive SIF mean that the crack is open. One established in this Fig. that the registered values of mode I SIF are about 0,109  $Mpa\sqrt{mm}$  for the first stem position according to 110° inclusion inclination and 0,116  $Mpa\sqrt{mm}$  for the second stem position. The third stem position gives a very weak SIF values.

So that 110° inclusion is the one which gives the most dangerous SIF, this is due firstly to the presence of the bony debris in the same axes load, so the load is applied directly in the same way of the inclusion inclination.

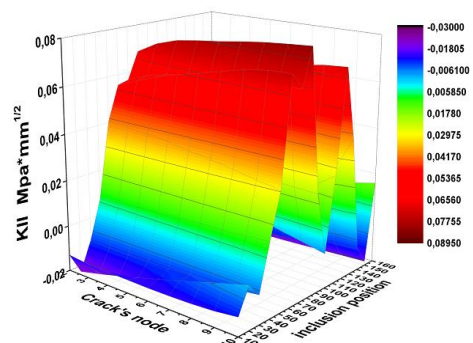


Fig. 18 Distribution of the KII along the crack front according to the inclusion position (Implant Normal)

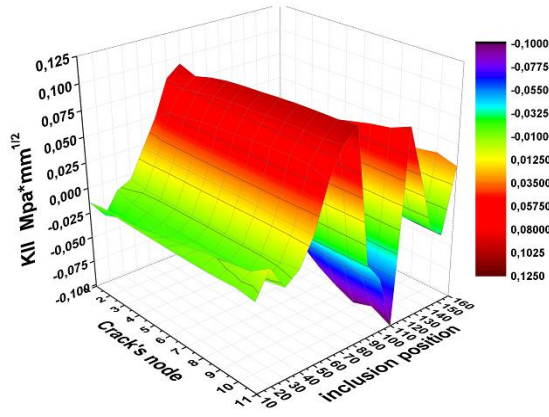


Fig. 19 Distribution of the KII along the crack front according to the inclusion position (Implant 23° behind)

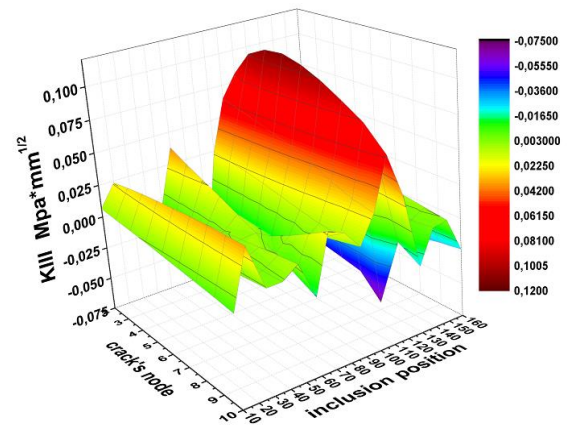


Fig. 22 Distribution of the KIII along the crack front according to the inclusion position (Implant 23° behind)

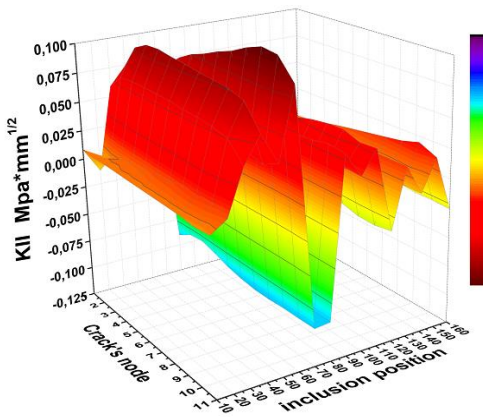


Fig. 20 Distribution of the KII along the crack front according to the inclusion position (Implant 23° forward)

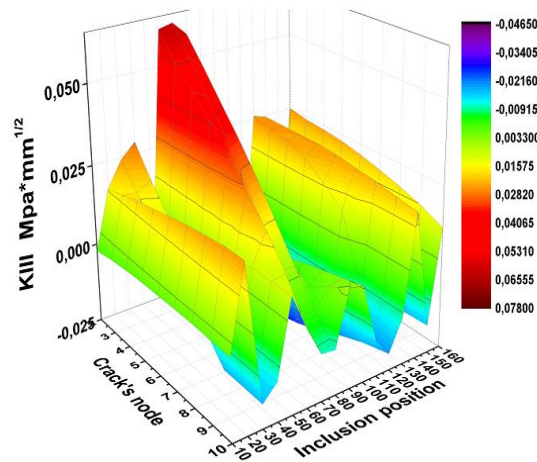


Fig. 23 Distribution of the KIII along the crack front according to the inclusion position (Implant 23° forward)

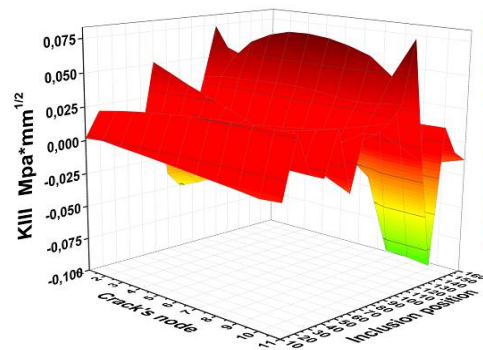


Fig. 21 Distribution of the KIII along the crack front according to the inclusion position (Implant normal)

These Fig. present the stress intensity factor with respect of the circumferential position of the bony inclusion. From the analysis of these Fig. in the three types of loading position, one can deduce that the interested results are found when the patient posture corresponds to 0° and +23°. At these positions the values of stress intensity factors are about  $0.1 \text{ Mpa} \cdot \sqrt{\text{mm}}$  when the inclusion position lies between 80° and 120°. At this position, the crack is open and can propagate in mix mode.

Furthermore, the (-23°) stem position, gives a negative mode I SIF, which indicates that the crack is closed and consequently this orientation does not expose the cement to any danger.

The combination of both crack's opening mode show that inclusion position between 80° and 120° gives an important SIF for both stem position 0° and 23° behind.

The Figs. 21-22 and 23 represent the disturbing KIII on the crack front according to the circumferential position of the bony inclusion, which varies between 10° and 160°. Again, we see clearly that the position which gives substantial values is 110° with an amplitude of 0.07 and 0.1  $\text{Mpa} \cdot \sqrt{\text{mm}}$  consecutively and corresponding to the position of the implant -23° and +23°.

#### 4. Conclusions

Orthopedic cement is a brittle material; in fact, the presence of a crack emanating from a bony inclusion disturb the stress distribution and can be the location of stress intensity, which can lead to the fracture of the cement and consequently the loosening of the THR. This study is carried out in the target to analyze using FEM the fracture

behavior of the orthopedic cement and the crack size effect on this behavior. From the obtained results one can deduce the following results:

- The loading and the geometry influence directly on the stress state of the orthopedic cement, the stress can be between 16 Mpa and 22 Mpa.
- The stem position, (the human body posture), has great effect on the stress state of the orthopedic cement. The first stem position and a radial inclusion position make cement in the highest stress state a head of the bony inclusion that can lead to the crack initiation at this position.
- When the bony inclusion is oriented toward the radial direction in the radial system, concentrates the stress a head of the inclusion.
- Stress position which provoke most risk correspond to 2nd position (23° forward).
- The default circumferential position is likely to cause the opening of the crack at the 110° position.
- The loading mode has a direct influence on the crack behavior, so in the presence of a crack emanating from an inclusion the +23° position leads to a significant level of damage, which gives interesting values of FIC in mode I, II, and III.
- The loading mode influences directly to the fracture behavior, so in the presence of the defect (inclusion + crack) at position +23° of stem leads to a significant level of damage, this provides interesting values CIF mode I, II, and III.

## References

- Abaqus 6.11 Documentation, *Abaqus Analysis User's Manual*.
- Benbarek, S., Bouiadjra, B., Achour, T., Belhouari, M. and Serier, B. (2007), "Finite element analysis of the behaviour of crack emanating from microvoid in cement of reconstructed acetabulum", *Mater. Sci. Eng.*, **457**(1-2), 385-391.
- Benbarek, S., Bouiadjra, B.A.B., El Mokhtar, B.M., Achour, T. and Serier, B. (2013), "Numerical analysis of the crack growth path in the cement mantle of the reconstructed acetabulum", *Mater. Sci. Eng. C*, **33**(1), 543-549.
- Benouis, A., Boulenuar, A., Benseddiqu, N. and Serier, B. (2015), "Numerical analysis of crack propagation in cement PMMA: application of SED approach", *Struct. Eng. Mech.*, **55**(1), 551-558.
- Bergman, G., *J. Biomech.*, **26**, 969-990.
- Bergmann, G.G., Deuretzbacher, G., Heller, F., Graichen, A., Rohlmann, J.S. and Duda, G.N. (2001) "Hip contact forces and gait patterns from routine activities", *J. Biomech.*, **34**(7), 859-871.
- Bouziane, M.M., Moulgada, A., Djebbara, N., Sahli, A., Bachir Bouiadjra, B. and Benbarek, S. (2016), "Effect of the residual stresses at the stem-cement interface on the mechanical behaviour of cemented hip femoral", *J. Eng. Res. Afr.*, **17**, 54-63.
- Bouziane, M.M., Salah, H., Benbarek, S., Bachir Bouiadjra, B. and Serier, B. (2015), "Finite element analysis of the mechanical behaviour of a reinforced PMMA-based hip spacer", *Adv. Mater. Res.*, **1105**, 36-40.
- Cherfi, M., Benbarek, S., Bachir, B. and Serier, B. (2016), "Numerical modeless of the damage, around inclusion in the orthopedic cement PMMA", *Struct. Eng. Mech.*, **57**(4), 717-731.
- Cintour Integral Evaluation, Section 11.4.2.
- Huiskes, R. (1993), "Failed innovation in total hip replacement", *Acta Orthop. Scand*, **64**(6), 699-716.
- Jamal-Omidi, M., Falah, M. and Davood, T. (2014), "3-D fracture analysis of cracked aluminum plates repaired with single and double composite patches using XFEM", *Struct. Eng. Mech.*, **50**(4), 525-539.
- Jasty, M., Maloney, W.J., Bragdon, C.R., O'Connor, D.O., Haire, T. and Harris, H.H. (1991), "The initiation of failure in cemented femoral components of hip arthroplasties", *J. Bone Joint Surg.*, **73**(4), 551-558.
- Jiang, S., Du, C. and Gu, C. (2014), "An investigation into the effects of voids, inclusions and minor cracks on major crack propagation by using XFEM", *Struct. Eng. Mech.*, **49**(5), 2014, 597-618.
- Maloney, W.J., Murali, J., Burke, D.W., O'Connor, D.O., Zalenski, C. and Braydon, E.B. (1989), "Biomechanical and histologic investigation of cemented total hip arthroplasties", *Clin. Orthop. Rel. Res.*, **249**, 129-140.
- Merckx, D. (1993), *Les Ciments Orthopediques Dans La Conception Des Protheses Articulaires*, Biomecanique et biomateriaux, Cahiers D'enseignement De La SOFCOT, Expansion Scientifique Francaise, **44**, 67-76.
- Nanda Kumar, M.R., Ramachandra, M.A, Smitha, G. and Nagesh, R.I. (2016), "XFEM for fatigue and fracture analysis of cracked stiffened panels", *Struct. Eng. Mech.*, **57**(1), 65-89.
- Naudin C. (2002), *Grumbach, Larousse Medicale*, Larousse.
- Ouinias, D., Bachir Bouiadjra, B., Serier, B., Benderdouche, N. and Ouinias, A. (2009), *Comput. Mater. Sci.*, **45**, 443-448.
- Pauwels, F. (1965), *Gesammelte Abhandlungen Zur Funktionellen Anatomie Des Bewegung-Sapparates*, Springer Verlag, Berlin, Germany.
- Pauwels, F. (1973), *Atlas Zur Biomechanik Der Gesunden Und Kranken Hufte*, Springer Verlag, Berlin, Germany.
- Poitout, D. *Biom'Ecanique Orthop'Edique*, Edition Masson.
- Pustoch, A. (2009), "Normal and osteoarthritic hip joint mechanical behaviour: A comparison study", *Med. Biol. Eng. Comput.*, **47**(4), 375-383.
- Sahlia, A., Benbareka, S., Wayneb, S., Bouiadjraa, B.A.B. and Serier, B. (2014), "3D crack behavior in the orthopedic cement mantle of a total hip replacement", *Appl. Bion. Biomech.*, **11**(3), 135-147.
- Serier, B., Zouambi, L., Bouziane, M.M., Benbarek, S. and Bouiadjra, B.B. (2016), "Properties and characterization of modern materials simulation of a crack emanating from a microvoid in cement of a reconstructed acetabulum", *Adv. Struct. Mater.*, **33**, 31-42.
- Tong, J. and Wong, K.Y., *Mixed Mode Fracture in Reconstructed Acetabulum*, Department of Mechanical and design Engineering, University of Portsmouth, Portsmouth, U.K.
- Yoshidaa, H., Fausta, A., Wilckensa, J., Kitagawaa, M., Fettob, J. and Edmund, Y.S. (2006), "Three-dimensional dynamic hip contact area and pressure distribution during activities of daily living", **39**(11), 1996-2004.
- Zagane, M.E.S., Smail, B., Abderahmane, S., Bouiadjra, B.B. and Serier, B. (2016), "Numerical simulation of the femur fracture under static loading", *Struct. Eng. Mech.*, **60**(3), 405-412.